

Ni-P-SiC composite coatings electroplated on carbon steel assisted by mechanical attrition

Zhaoxia PING ^{1)*}, Guoan CHENG ¹⁾ and Yedong HE ²⁾

1) Key Laboratory of Beam Technology and Material Modification of Ministry of Education, College of Nuclear Science and Technology, Beijing Normal University, Beijing 100875, China

2) Beijing Key Laboratory for Corrosion, Erosion and Surface Technology, University of Science and Technology Beijing, Beijing 100083, China

Manuscript received 27 October 2009; in revised form 14 December 2009

In this work, Ni-P-SiC composite coatings were electroplated on carbon steel substrate assisted by mechanical attrition (MA). The MA action was conducted by dispersing glass balls on the cathodic surface, vibrating in the horizontal direction. The experimental results show that, under the assistant of MA action, the adhesion of Ni-P-SiC coating on the steel substrate can be improved effectively, and the Ni-P-SiC coatings exhibit a crystallized structure and Ni-P matrix can combine tightly with SiC particles, and the hardness and corrosion resistance of these coatings increase markedly. During heat treatment, the defects produced in conventional Ni-P-SiC composite coatings can be avoided assisted by MA action. Both of the wear resistance and corrosion resistance of these coatings can be improved further.

KEY WORDS Ni-P-SiC composite coating; Electroplating; Mechanical attrition

1 Introduction

The composite coatings are expected to have tailor-made properties for some specific applications. Recent progress in electroplating is the co-deposition of SiC particles into Ni-P coatings to enhance the hardness and/or wear resistance of the deposits^[1-3]. Broszeit found that mechanical properties, such as hardness, strength and elastic modulus can be increased with increasing content of SiC particles in the composite coating^[4]. Xinmin and Zongang suggested that the SiC particles can increase the hardness of a composite coating and improve the resistance to abrasion, but a hard and stable matrix is necessary to support them^[5]. Microscopically, what really happens in such composite coatings is not well understood and needs further investigation.

Recently, a new thought of electroplating assisted by MA has been paid much more attention^[6,7]. Ni coating was deposited on carbon steel by a mechanical attrition enhanced electroplating process^[6]. It is shown that MA action has significant effects on the microstructure and the characteristics of electroplated Ni coating. It is proved that

*Corresponding author. Tel.:

E-mail address:

the growth of the grains is hindered under the MA action and the nucleation of Ni grains processes at a high rate. Thus the Ni coating deposited has smooth surface morphology, refined grain size, pore-free, and increased microhardness and excellent corrosion resistance. MA has been also applied to improve the electroless plating process in the magnesium alloy. The results indicated that an alloyed layer forms at the interface of Ni-P coating and magnesium alloy. The Ni-P coating becomes smooth, compact, has refined grains, and is free of cracks and pores. The phase of the Ni-P coating transformed from amorphous to crystalline. Consequently, the coating adhesion, hardness and corrosion resistance have been improved significantly.

This paper attempts to incorporate SiC particles into a Ni-P alloy matrix by electroplating assisted with MA and to study the effect of MA action on the microstructure and properties of the composite Ni-P-SiC coatings.

2 Experimental Procedure

The device to electroplate composite Ni-P-SiC coatings assisted by MA action is schematically shown in Fig.1. The plating bath was placed on the top of a vibrator. The vibrator provided a sinusoidal vibration of 1 mm amplitude and 4.5 Hz frequency in the horizontal direction. Samples to be plated were made of carbon steel and had dimensions of 20 mm×10 mm×2 mm. Two carbon steel samples were mounted in epoxy resin worked as the cathode. The sample surfaces were ground with SiC papers to 1200-grit finish. After installing the cathode, glass balls with density of 2.2 g/cm³ and diameters of 1, 5 and 7 mm were dispersed on the cathode surface. When the plating bath was vibrated, these glass balls rolled horizontally forth and back and provided mechanical attrition action on the surfaces of coatings during the plating process. The anode was a high-purity nickel plate with an effective surface area of 30 mm×20 mm and parallel to the cathode surface, as illustrated in Fig.1. The DC power turned on when the vibrator moved horizontally. A standard nickel Watts' solution was used as the basic plating solution, in which SiC powder of size 2-3 μm was mixed and stirred magnetically for 2 h and then agitated ultrasonically for 20 min just before electroplating. The agitation was expected to disperse SiC particles uniformly in the electroplating bath. The composition of the plating solution and plating parameters are listed in Table 1. Electroplating all carried out at 70 °C for 20 min, which yielded a coating thickness larger than 20 μm. Some samples were annealed at 400 °C for 1 h to investigate the influence of heat treatment on the microstructure and properties of such composite Ni-P-SiC coatings.

X-ray diffraction (XRD, PW3710, Philips) were conducted to characterize crystal structures of as-deposited coatings. The surface and cross-section morphologies of the coatings were examined by scanning electron microscopy (SEM, JSM-6480LV). Chemical compositions of the coatings were analyzed by the EDS attached in the SEM. Hardness was

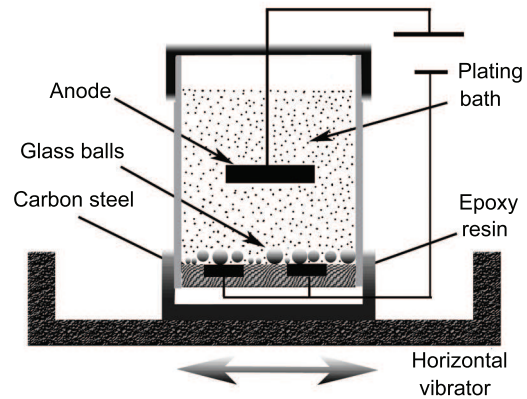


Fig.1 Schematic illustration set-up of electroplating assisted by MA.

Table 1 Composition of the plating solution and plating parameters

Plating solution composition (g/L)		Electroplating parameter	
NiSO ₄ ·6H ₂ O	250	pH	3
NiCl ₂ ·6H ₂ O	15	Temperature	70 °C
NaCl	15	Current density	25 mA/cm ²
H ₃ BO ₃	30	Plating time	20 min
H ₃ PO ₃	6	Anode	Ni (6 cm ²)
NaH ₂ PO ₂ ·H ₂ O	20	Cathode	Carbon steel (4 cm ²)
SiC (2–3 μm) (g/l)	0, 5, 10		

measured using a digital microhardness tester (HVS-1000) with a load of 2.94 N and a duration time of 20 s. At least ten indents were performed to gain the average hardness value for each sample.

The polarization curves were measured in a three-electrode cell using a PS-168B electrochemical measurement system. A platinum electrode, a saturated calomel electrode (SCE) and coated sample were used as counter electrode, reference electrode and working electrodes, respectively. The measurements were carried out in a 3.5%NaCl solution at room temperature with a sweep rate of 0.1 mV/s. The electrochemical impedance spectroscopy (EIS) tests were performed on a galvanic-chemistry Workstation (CHI660C, Shanghai) in 3.5% NaCl solution at room temperature by using a traditional three-electrode electrochemical cell as same as that to measure the polarization curves. During the electrochemical tests, only an area of 1 cm² of the surface of coatings exposed in solution worked as working electrode. The EIS spectra were measured over a frequency range of 10 mHz–100 kHz with an applied AC perturbation potential of 10 mV amplitude. The experimental results were analyzed on the basis of an equivalent circuit determined using a suitable fitting procedure described in Zsimpwin software.

3 Experimental Results

3.1 Surface morphology

Fig.2 shows the typical difference of surface SEM morphologies of Ni-P-SiC coatings assisted with and without MA action electroplated respectively in a bath containing SiC of 10 g/L, at a current density of 25 mA/cm² for 20 min. It can be seen that the surface morphology of Ni-P-SiC coating assisted with MA action is quite different from that without MA action, and many “volcanic vent” like clusters are formed in the surface of

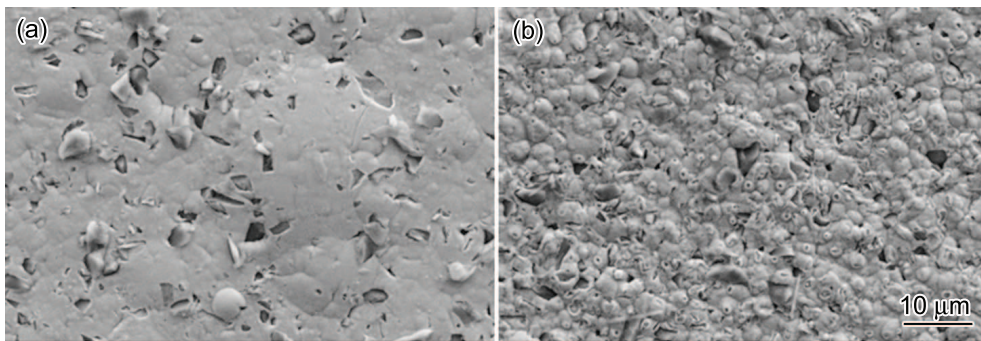


Fig.2 Surface SEM morphologies of Ni-P-SiC coatings assisted without (a) and with (b) MA action electroplated in a bath containing SiC of 10 g/L at current density of 25 mA/cm² for 20 min.

Ni-P-SiC coating. This demonstrates that assisted with MA action, the mechanism to plating Ni-P-SiC coating is changed completely.

The pictures in Fig.3 shows the surface SEM morphologies of electroplated Ni-P-SiC coatings on carbon steel at the current density of 25 mA/cm^2 for 20 min. As no SiC in the plating bath, the coating exhibits a typical “cauliflower-like” morphology (Fig.3a) with a nano-crystallized structure. This phenomenon is consistent with our pervious results. Comparing Fig.3b with Fig.3d, it can be found that the SiC content in the plating bath (or in coating) can change the surface morphology of Ni-P-SiC coatings greatly. It can be seen that the surface morphology of Ni-P-SiC coating plated in the bath containing SiC of 5 g/L with the assistance of MA action is quite similar with that plated in the bath containing SiC of 10 g/L without the assistance of MA action (Fig.3c). However, as plated in the bath containing SiC of 10 g/L with the assistance of MA action, many “volcanic vent” like clusters are formed in the surface of Ni-P-SiC coating. These results reveal that the contents of SiC in plating baths, in other words, the contents of SiC in coatings, can markedly influence the mechanism to electroplate Ni-P-SiC coatings with the assistance of MA action.

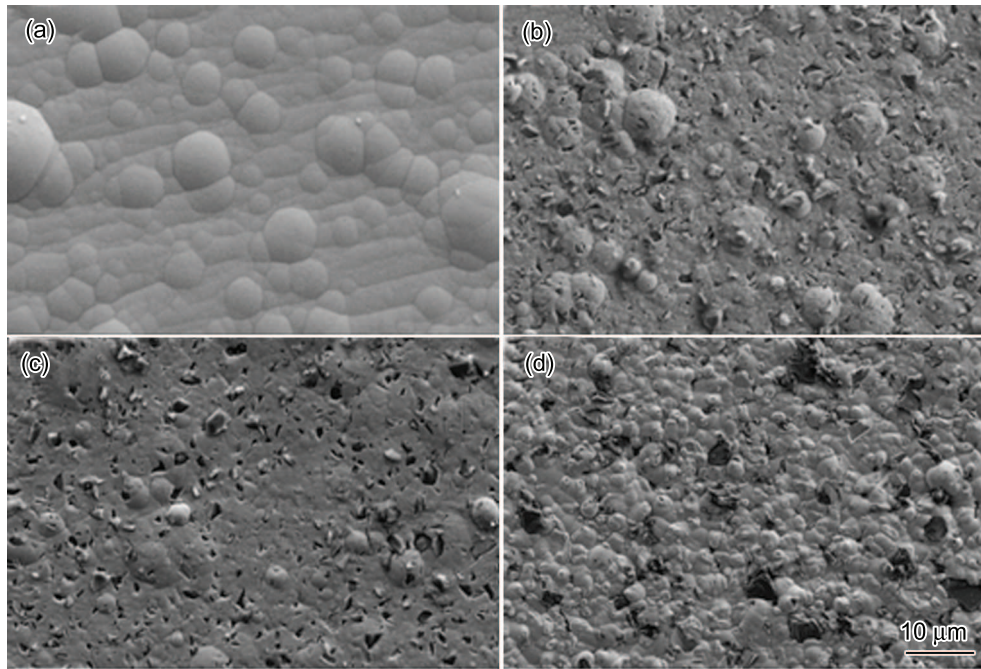


Fig.3 Surface morphologies of electroplated Ni-P-SiC coatings on carbon steel at the current density of 25 mA/cm^2 for 20 min: (a) with MA, SiC: 0 g/L; (b) with MA, SiC: 5 g/L; (c) without MA, SiC: 10 g/L; (d) with MA, SiC: 10 g/L.

Fig.4 shows the SEM images of cross-sections of Ni-P-SiC coatings electroplated in baths containing different SiC contents without and with the assistance of MA action at the current density of 25 mA/cm^2 for 20 min, respectively. It can be seen that the several effects of MA action on the structure of Ni-P-SiC coatings are generated. Firstly, the interface at the Ni-P-SiC coating/carbon steel substrate is quite different without and with MA action. In former case, the interface is very clear, even cracked after polishing;

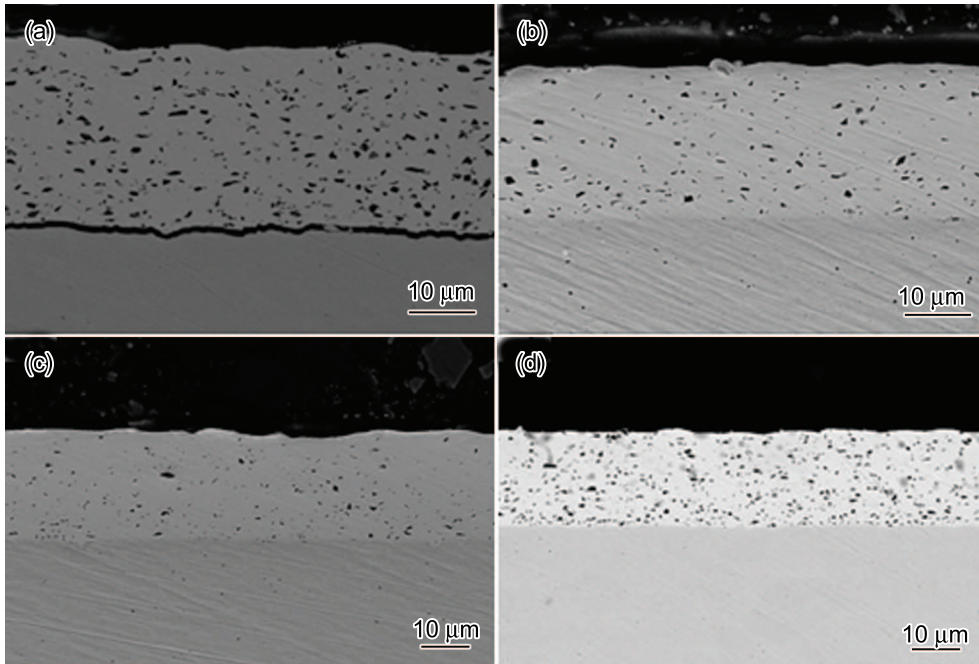


Fig.4 Cross-sectional SEM images of Ni-P-SiC coatings electroplated at the current density of 25 mA/cm^2 for 20 min. respectively: (a) without MA in a bath containing SiC of 10 g/L, (b) with the assistance of MA action in a bath containing SiC of 10 g/L, (c) with the assistance of MA action in a bath containing SiC of 5 g/L and (d) with the assistance of MA action in a bath containing SiC of 10 g/L.

while in the latter case, the interface is ambiguous, which means the adhesion of the coating with substrate is enhanced obviously by MA action. Secondly, SiC content in Ni-P-SiC coatings is decreased with MA action and increased with increasing the SiC content in plating bath. Thirdly, the thickness of Ni-P-SiC coatings is reduced by MA action.

Fig.5 shows the influence of heat treatment on the surface morphologies of Ni-P and Ni-P-SiC coatings plated on carbon steel without and with MA action respectively. It can be seen that after heat treatment at 400°C for 1 h, many obvious pores are formed in the Ni-P coating without MA action (Fig.5a), while no obvious pores can be observed in the Ni-P coating with MA action (Fig.5b), which means MA action can reduce the defects in the Ni-P coatings after heat treatment. Similarly, after heat treatment, the defects, such as pores, in Ni-P matrix of Ni-P-SiC coatings can be effectively reduced as well by MA action (Fig.5d). It could be suggested that these phenomenon should be generated in similar mechanism.

3.2 Phase analysis

Fig.6 shows the XRD patterns of Ni-P-SiC coatings electroplated with and without MA action. It is demonstrated that the Ni-P-SiC coating electroplated in traditional way is composed of amorphous Ni-P matrix and SiC crystal particles, while the Ni-P-SiC coating electroplated by assistance of MA action is composed of a matrix of Ni crystal phase and SiC crystal particles. It is proved again that when the content of P is about 8%, the phase of the Ni-P coating can transform from amorphous to crystalline by the action of MA. The EDS analysis results indicate that the P content in the electroplated Ni-P coating is about

6.9 wt pct, whereas it is about 8.1 wt pct in the coating assisted by MA action. So, MA action can increase the P content in coating slightly.

3.3 Microhardness

Fig.7 shows both influences of SiC content in baths and heat treatment on the hardness of Ni-P-SiC coatings electroplated by the assistance of MA action. It can be seen that the hardness of the Ni-P-SiC coatings is increased with the SiC content in baths, but heat treatment at 400 °C for 1 h can enhance tremendously the hardness of such Ni-P-SiC coatings. Combining the roles of SiC particles (SiC 10 g/L) and heat treatment, the

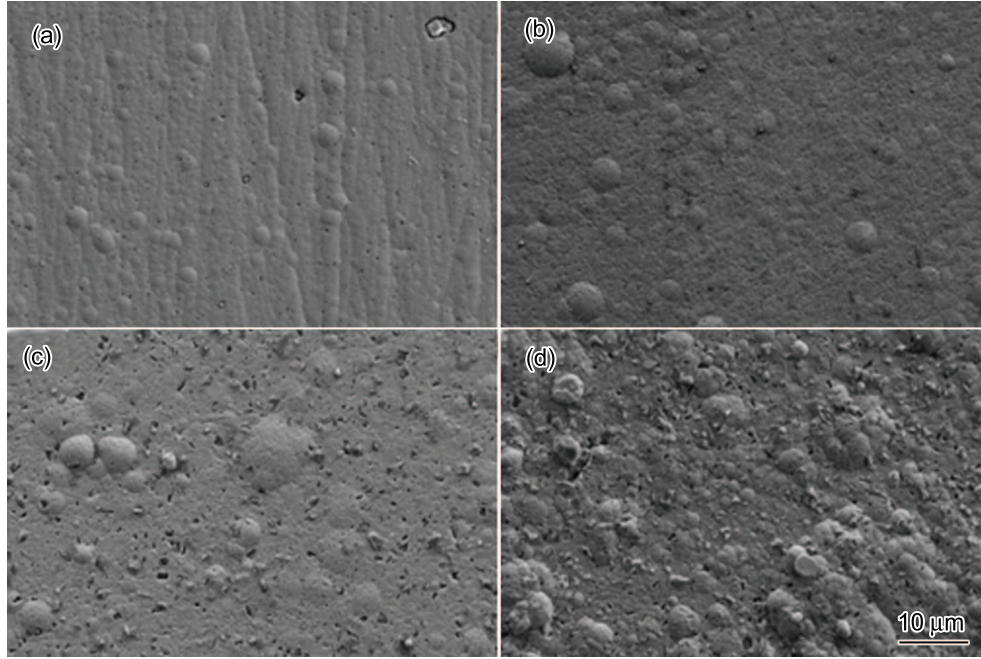


Fig.5 Surface morphologies of Ni-P and Ni-P-SiC coatings plated on carbon steel without (a, c) and with MA (b, d) action and heat treated at 400 °C for 1 h respectively.

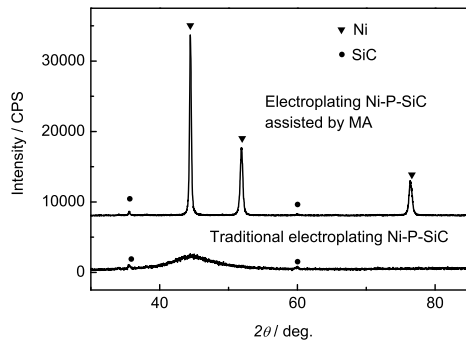


Fig.6 XRD patterns of electroplated and electroplated by MA Ni-P-SiC coatings on carbon steels.

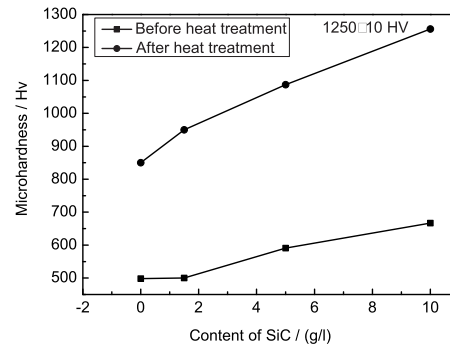


Fig.7 Influences of SiC content in baths and heat treatment on the hardness of Ni-P-SiC coatings electroplated by the assistance of MA action.

hardness of the Ni-P-SiC coatings can reach as high as 1256 ± 10 HV, which is, so far, the highest value among all the hardness of plating Ni-P-SiC coatings reported literatures.

3.4 Corrosion resistance

Fig.8 shows the polarization curves of carbon steel and Ni-P-SiC coatings electroplated with and without the assistance of MA action in 3.5% NaCl solution at room temperature. It can be seen that the corrosion potential of Ni-P-SiC coating electroplated with the assistance of MA action shift to a positive value comparing with the Ni-P-SiC coating electroplated in traditional way, which means that the structure of Ni-P-SiC coating becomes very compact under the action of MA, so that the galvanic corrosion resistance between the Ni-P-SiC coating and carbon steel is improved significantly.

Fig.9a shows the EIS data presented in the Nyquist format measured in 3.5% NaCl solution at room temperature by using a traditional three-electrode electrochemical cell, in which, a platinum electrode, a saturated calomel electrode (SCE) and sample were used as counter electrode, reference electrode and working electrodes, respectively. Theoretically, the high-frequency impedance arc is attributed to the processes occurring at the electrode-electrolyte interface and the diameter of the arc can be regarded as the polarization resistance (R_t) at this interface^[8]. An equivalent circuit as shown in Fig.9b for the working electrode is proposed, in which, R_s is a solution resistance; Q_{dl} is an electrical double layer capacitance at the interface of electrode and electrolyte; R_t is a polarization resistance; and W is a Warburg component. The Warburg impedance is usually observed at low frequencies in electrochemical experiments due to the concentration polarization induced by a sluggish diffusion process^[9]. The circuit parameters were approximately determined by fitting the experimental data with the equivalent circuit and tabulated in

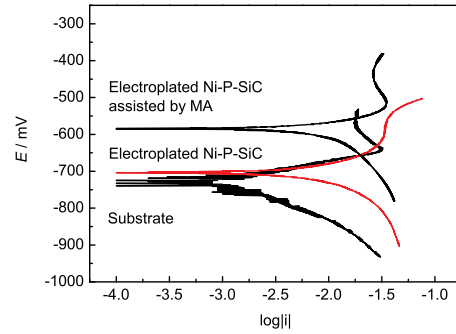


Fig.8 Polarization curves of carbon steel substrate, electrodeposited Ni-P-SiC coating and electroplated Ni-P-SiC coating assisted by MA in 3.5% NaCl solution at room temperature.

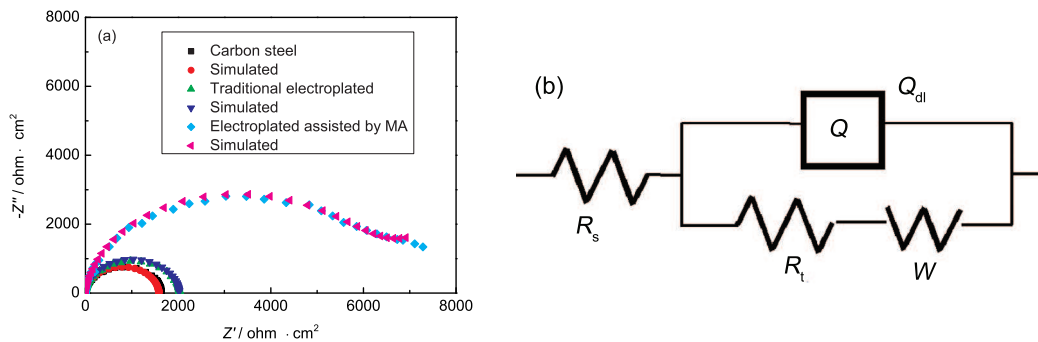


Fig.9 (a) Nyquist plots for carbon steel substrate, conven electrodeposited Ni-P-SiC coating and electroplated Ni-P-SiC coating assisted by MA in 3.5% NaCl solution at room temperature; (b) equivalent circuit for simulating the EIS data.

Table 2 Fitting EIS data of the carbon steel substrate, electrodeposited Ni-P-SiC coating and the electroplated Ni-P-SiC coating assisted by MA in 3.5% NaCl solution

Sample	Substrate	Traditional electroplating Ni-P-SiC	Electroplating Ni-P-SiC assisted by MA
$R_s/\Omega\cdot\text{cm}^2$	0.80	0.91	0.84
$R_t/\Omega\cdot\text{cm}^2$	1618	1999	6586
$Q_{dl}/(\text{F}/\text{cm}^2)$	$1.68\cdot 10^{-4}$	$1.73\cdot 10^{-4}$	$9.06\cdot 10^{-5}$
n_{dl}	0.9803	0.9796	0.9447

Table 2. For comparison, the simulated curves are also shown in Fig.9a. In Table 2, factor n_{dl} represents the Q_{dl} power, which is usually between 0.5 and 1^[10]. When $n_{dl}=1$, a Q_{dl} is equivalent to an ideal capacitor. The experimental results show that the polarization resistance (R_t) of the Ni-P-SiC coating electroplated by the assistance of MA action is higher than that electroplated traditionally. Therefore, it is proved again that the corrosion resistance of Ni-P-SiC coating can be significantly improved by the assistance of MA action.

4 Discussion

From above mentioned experimental results, it can be seen that both of the structure and properties of Ni-P-SiC composite coatings are significantly changed by the assistance of MA action. Comparing with the effects of MA action produced in plating Ni-P coating, the effects of MA action produced in the present research have some new characteristics, as discussed in the following.

Firstly, the MA action in plating Ni-P-SiC composite coatings is generated by both of glass balls and SiC particles, which is not as same as that generated only by glass balls in plating Ni-P coating. This MA action not only induces plastic deformation, but also induces slight abrasion, which is beneficial to clean the steel surface, leading to the formation of new structure at coating/steel interface, as shown in Fig.4b, c and d. Therefore, the adhesion of Ni-P-SiC coating with steel substrate can be improved effectively. In another hand, however, this MA action can supply a kinetic energy on SiC particles and wear the coating, so, both of the SiC content in coating and the thickness of coating are decreased, as shown in Fig.4.

Secondly, the Ni-P matrix in Ni-P-SiC composite coating is transformed from an amorphous state to a crystal line state by the assistance of MA action, which is similar to the phenomenon happened in Ni-P coating plated by the assistance of MA action^[11]. Generally, the crystallization and phase transformation behavior of electroplating Ni-P coating happens during thermal processing and the driving force for crystallization comes from thermal energy^[12–17]. However, the present work proves that MA action can generate crystallization of Ni-P matrix in Ni-P-SiC coating as well, The Ni-P-SiC coating deposited by the assistance of MA action exhibits two phases of Ni and SiC without the phase of Ni_3P , as shown in Fig.6, which indicates that the energy produced by MA action is not sufficient enough for Ni and P atoms to diffuse together forming a Ni_3P phase. The detailed thermodynamics analysis for this effect is reported in a previous publication^[11].

Thirdly, the combination of Ni-P matrix with SiC particles can be enhanced by MA action markedly. This effect can be explained by Fig.10. In traditional electroplating, current density concentrates lightly at the edges of Ni-P matrix contact with SiC particles, grow up gradually (Fig.10a), and cover the SiC particles finally (Fig.10b). Defects such

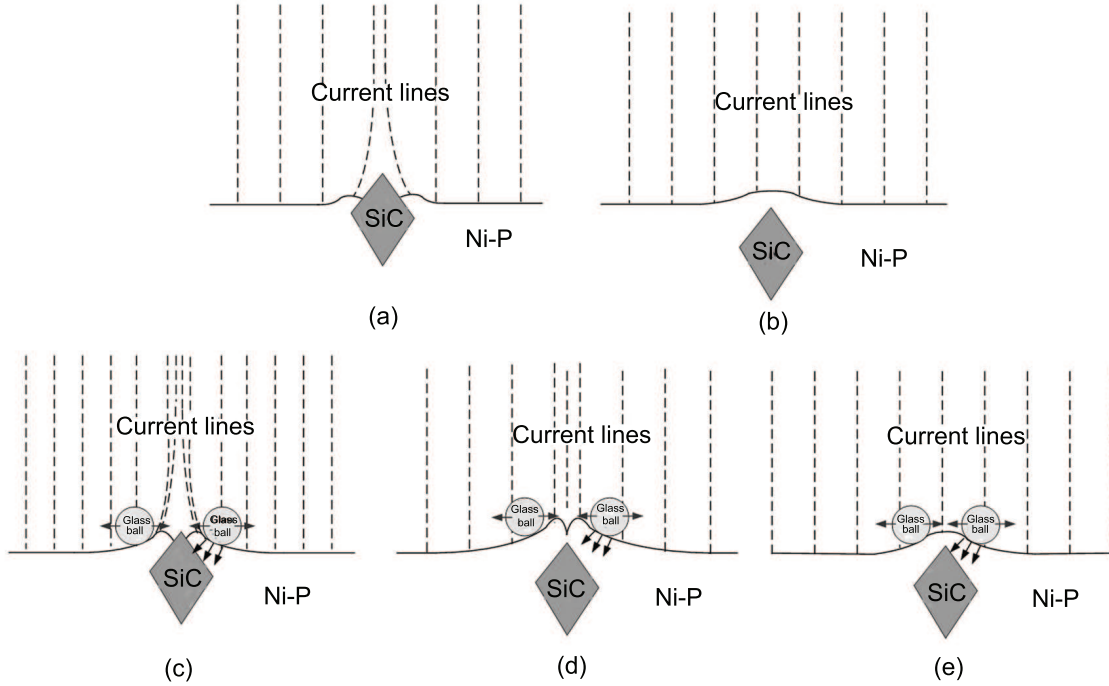


Fig.10 Model on the formation of Ni-P-SiC composite coatings: (a, b) traditional electroplating; (c, d, e) electroplating assisted by MA action.

as pores and crevices form easily around the SiC particles. So, the combination of Ni-P matrix with SiC particles in such coatings is not well. But in the case with MA action, combining both roles of Ni-P growth produced by current density concentration and plastic deformation produced by MA action, the edges of Ni-P matrix contacted with SiC particles are extracted as “volcanic vents” (Fig.10c), the “volcanic vents” are gradually sealed up (Fig.10d) and are smoothed finally by MA action (Fig.10e). So, the defects, such as pores and cracks are difficult to form around the SiC particles, showing an excellent combination of Ni-P matrix with SiC particles. Therefore, Ni-P-SiC composite coatings can be effectively strengthened by the SiC particles, both of hardness and corrosion resistance of Ni-P-SiC composite coatings can be significantly improved as well.

Finally, the defects produced in conventional Ni-P-SiC composite coatings during heat treatment can be avoided in these coatings assisted by MA action. So that, both of wear and corrosion resistance of these coatings can be improved further. This beneficial effect can attributed to the crystallization of Ni-P matrix in Ni-P-SiC composite coatings produced by MA action. Consequently, the phenomenon of volume shrinkage of traditional Ni-P-SiC coating happened in heat treatment can be avoid in the Ni-P-SiC composite coatings produced by MA action, so, the galvanic corrosion between the coating and steel substrate can be inhibited effectively. Owing to the formation of Ni_3P phase in the Ni-P-SiC composite coatings in heat treatment, the hardness and wear resistance of such coatings are increased tremendously.

5 Conclusions

In summary, a novel coating process-the mechanical assistant electroplating-has been

developed to deposit Ni-P-SiC coatings on carbon steel. Under the assistant of MA action, the adhesion of Ni-P-SiC coating with steel substrate can be improved effectively, the Ni-P matrix in Ni-P-SiC coatings exhibits a crystallized structure and Ni-P matrix can combine tightly with SiC particles, and the hardness and corrosion resistance of these coatings increase markedly. During heat treatment, the defects produced in conventional Ni-P-SiC composite coatings can be avoided in these coatings assisted by MA action. So that, both of the wear resistance and corrosion resistance of these coatings can be improved further. Therefore, it is suggested that the mechanical assistant electroplating technique might has wide application in industries.

Acknowledgements—The work was financially supported by the National Natural Science Foundation of China (No.50671006).

REFERENCES

- [1] M.R. Kalantary, K.A. Holbrook and P.B. Wells, *Trans Inst Metal Finish* **71** (1993) 55.
- [2] K.L. Lin and P.J. Lai, *Plat Surf Finish* **76** (1989) 48.
- [3] N. Feldstein, T. Lancsek, R. Barras, R. Spencer and N. Bailey, *Prod Finish* **44** (1980) 65.
- [4] E. Broszeit, *Thin Solid Films* **95** (1982) 133.
- [5] H. Xinmin and D. Zongang, *Trans Inst Metal Finis* **70** (1992) 84.
- [6] Z. Ning, Y. He and W. Gao, *Surf Coat Technol* **202** (2008) 2139.
- [7] Y. He, H. Fu, X. Li and W. Gao, *Scr Mater* **58** (2008) 504.
- [8] J. Gamby, P.L. Taberna, P. Simon, J.F. Fauvarque and M. Chesneau, *J Power Sources* **101** (2001) 109.
- [9] Jung-Suk Yoo and Su-Moon Park, *Anal Chem* **73** (2001) 4060.
- [10] X. Zhang, S.O. Pehkonen, N. Kocherginsky and G.A. Ellis, *Corros Sci* **44** (2002) 2507.
- [11] Z. Ping, Y. He, C. Gu and T. Zhang, *Surf Coat Technol* **202** (2008) 6023.
- [12] Z. Guo, K.G. Keong and W. Sha, *J Alloy Compd* **358** (2003) 112.
- [13] J.N. Balaraju, T.S.N. Sankara Narayanan and S.K. Seshadri, *Mater Res Bull* **41** (2006) 847.
- [14] M. Palaniappa and S.K. Seshadri, *Mater Sci Eng A* **638** (2007) 460.
- [15] S. Budurov, V. Fotty and S. Toncheva, *Mater Sci Eng A* **133** (1991) 452.
- [16] I. Baskaran, T.S.N. Sankara Narayanan and A. Stephen, *Mater Chem Phys* **99** (2006) 117.
- [17] N.M. Martyak and K. Drake, *J Alloy Compd* **312** (2000) 30.